Biophysical Journal Volume 78 January 2000 34–46

Theory of Lipid Polymorphism: Application to Phosphatidylethanolamine and Phosphatidylserine

Xiao-jun Li and M. Schick

Department of Physics, Box 351560, University of Washington, Seattle, Washington 98195-1560, USA

ABSTRACT We introduce a microscopic model of a lipid with a charged headgroup and flexible hydrophobic tails, a neutral solvent, and counter ions. Short-ranged interactions between hydrophilic and hydrophobic moieties are included as are the Coulomb interactions between charges. Further, we include a short-ranged interaction between charges and neutral solvent, which mimics the short-ranged, thermally averaged interaction between charges and water dipoles. We show that the model of the uncharged lipid displays the usual lyotropic phases as a function of the relative volume fraction of the headgroup. Choosing model parameters appropriate to dioleoylphosphatidylethanolamine in water, we obtain phase behavior that agrees well with experiment. Finally we choose a solvent concentration and temperature at which the uncharged lipid exhibits an inverted hexagonal phase and turn on the headgroup charge. The lipid system makes a transition from the inverted hexagonal to the lamellar phase, which is related to the increased waters of hydration correlated with the increased headgroup charge via the charge–solvent interaction. The polymorphism displayed upon variation of pH mimics that of the behavior of phosphatidylserine.

INTRODUCTION

Biological lipids in solution display several different lyotropic phases, and the implications this may have for biological function has been a subject of speculation for many years (Cullis et al., 1985; de Kruijff 1997). Lipid phase behavior depends upon several factors, some of which are intrinsic to the lipid architecture itself. For example, an increase in the length of the hydrocarbon tails brings about transitions from lamellar, L_α, to inverted hexagonal, H_{II}, phases (Seddon, 1990), whereas an increase in the volume of the headgroup brings about the reverse (Gruner, 1989). Other factors regulating phase behavior are externally controlled, such as temperature, solvent concentration, and solvent pH (Hope and Cullis, 1980; Seddon et al., 1983; Bezrukov et al., 1998). It is these factors that are the focus of this paper.

Lipid phase behavior has been addressed extensively by the construction of phenomenological free energy functions, which contain terms describing, inter alia, bending, hydration, and interstitial energies (Helfrich, 1973; Kirk et al., 1984; Rand and Parsegian, 1989; Kozlov et al., 1994). Such approaches, which obtain their several parameters from experimental measurement of various quantities, are quite useful, particularly in correlating phase behavior with other thermodynamic properties. Nonetheless, it would clearly be desirable to derive all thermodynamic quantities, including the phase behavior, by applying statistical mechanics to a microscopic model of the system. In addition to simplifying the description considerably, such approaches would correlate phase behavior with the architectural properties of the lipid itself and its solvent.

Analytic, mean-field approaches of statistical mechanics have been applied to anhydrous lipids to investigate behavior of increasing complexity. Such methods have been combined with realistic models of lipid tails to determine how the hydrocarbon chains pack in aggregates and in bilayers (Marcelja, 1974; Gruen, 1981, 1985; Ben-Shaul et al., 1985; Fattal and Ben-Shaul, 1994). Results for the bilayer are in good agreement with molecular dynamic simulation (Tieleman et al., 1997). These methods have shown that, in a neutral, anhydrous system, the entropy of the lipid tails always favors the H_{II} over the L_α phase, and that a change in area per headgroup could bring about a transition between them (Steenhuizen et al., 1991).

Aggregates, such as the lipid bilayer, in the presence of solvent have also been considered within the mean-field approach applied to lattice models (Leermakers and Scheutjens, 1988). In addition to the tails, one must now model the solvent and the headgroups, and phosphatidylcholine and phosphatidylserine headgroups are among those that have been described (Meijer et al., 1994). The method is flexible and has been applied to many different systems, including bilayers with trans-membrane guest molecules (Leermakers et al., 1990). Results are quite good, with the exception that the local volume fraction of solvent inside the bilayer is rather large, several orders of magnitude greater than that observed in experiment (Jacobs and White, 1989). Lattice models, however, are not well-suited to the description of transitions between phases of different symmetry.

It would be extremely useful to have available a relatively simple and tractable model of lipids that was capable, at least, of describing the effect of their architecture upon their phase behavior. With this in hand, one could, inter alia, examine the various bicontinuous phases to determine their stability or metastability (Shyamsunder et al., 1988), and to

Received for publication 28 January 1999 and in final form 20 October 1999.

Address reprint requests to Xiao-jun Li, University of Washington, Department of Physics, Box 351560, Seattle, WA 98195-1560. Tel.: 206-543-9697; Fax: 206-685-0635; E-mail: li@phys.washington.edu.

0006-3495/00/01/34/13 $2.00

explicate the reasons they facilitate the crystallization of membrane proteins (Landau and Rosenbusch, 1996). Further, one could explore mixtures of lamellar- and nonlamellar-forming lipids to determine the role that the latter play in lipid–protein interactions (Epand, 1998), membrane fusion (Markin et al., 1984; Siegel, 1993), and membrane function (Hui, 1997), all areas in which the importance of their presence has been indicated.

Toward this end, a model system of solvent and monoacyl lipid embedded in a continuous space was recently introduced. Its phase diagram was obtained by solving the mean-field theory exactly (Müller and Schick, 1998). It displayed both L_α and H_{II} phases, so that the transition between them could be studied as a function of lipid architecture. The dependence of the transition on the architectural parameters, length of tail, and volume of headgroup, was that observed in experiment. However, the fraction of solvent within the bilayers was again too large.

In this paper, we use a model of a lipid computationally more tractable than that used by Müller and Schick: one whose hydrocarbon tails are modeled as flexible chains rather than within the rotational isomeric states framework used earlier (Flory, 1969; Mattice and Suter, 1994). We first study the model with an uncharged headgroup. Its phase behavior, both with respect to variations in architecture and in solvent concentration, is as expected, and in agreement with experiment. In particular, choosing model parameters appropriate to dioleoylphosphatidylethanolamine (DOPE), we obtain a phase diagram similar to that observed (Gawrisch et al., 1992; Kozlov et al., 1994). We extract the variation with temperature and solvent concentration of the lattice parameter of the inverted hexagonal phase, and compare it to experiment (Tate and Gruner, 1989; Rand and Fuller, 1994). The agreement is excellent. We also find that the concentration of solvent within the bilayer is vanishingly small. We then allow the headgroup to be negatively charged. We introduce counter ions into the system, include the Coulomb interaction between all charges, and also a short-ranged interaction between charges and neutral solvent, an interaction that models the thermally averaged interaction between charges and the dipole of water. As the charge on the headgroup is turned on, the L_α phase is stabilized with respect to the H_{II}. In effect, as the charge on the headgroup increases, so too do the waters of hydration. In addition, the counter ions that are attracted to the headgroup are also enlarged by their own waters of hydration. It is the totality of these waters that effectively increases the headgroup volume and therefore stabilizes the lamellar phase.

The paper is organized as follows. In the next section, we introduce the model for the charged lipid, the solvent, and counter ions, specify all the interactions between them, and set up the partition function of the system. In the Theory section, we first derive the self-consistent field theory for it. At the heart of the theory are four self-consistent equations for the electrostatic potential of the system and the three effective fields that determine the headgroup, tail, and solvent densities. One of these self-consistent conditions is simply the nonlinear Poisson–Boltzmann equation. We then expand all functions of position into a complete set of functions having a specified space–group symmetry, and rewrite the self-consistent equations in terms of the coefficients of these expansions. These equations are solved numerically, and the free energies of the various phases computed. A comparison of the free energies yields the phase diagram.

In the Results section, we first present the phase diagram for the neutral lipid as a function of temperature and one architectural parameter. We include here only the classical phases, lamellar, inverted and normal hexagonal, and inverted and normal body-centered-cubic, as well as the disordered phase. For the remainder of this subsection, we choose an architecture such that the anhydrous, neutral lipid orders into the H_{II} phase. Results for the system in the presence of a neutral solvent, along with comparisons to experiment, are presented next.

In the next subsection, we consider the charged lipid. We choose a water concentration such that the neutral lipid remains in the H_{II} phase. By varying the counter ion concentration, we turn on the charge on the headgroup, and thus all Coulomb interactions, and all short-ranged interactions between charges and solvent. We find that the L_α is indeed stabilized with respect to the H_{II} phase, in agreement with experiment (Hope and Cullis, 1980; Bezrukov et al., 1998).

THE MODEL

We consider a system composed of charged lipids, neutral solvent, and counter ions in a volume V. There are n_L lipids, each of which consists of a head, with volume v_h, and two equal-length, completely flexible tails each consisting of N segments of volume v_t. Each lipid tail is characterized by a radius of gyration $R_g = (Na^2/6)^{1/2}$, with a the statistical segment length. The heads carry a negative charge $-eQ_h$. The solvent consists of n_s neutral particles of volume v_s, whereas the n_c counter ions have charge $+e$ and negligible volume, $v_c = 0$. There are five dimensionless densities that totally specify the state of the system; the number density of the headgroups, $\hat{\Phi}_h$, of the tail segments, $\hat{\Phi}_t$, and of the solvent, $\hat{\Phi}_s$, and the charge density of the headgroups, $e\hat{P}_h$, and of the counter ions, $e\hat{P}_c$. They can be written as

$$\hat{\Phi}_h(\mathbf{r}) = v_h \sum_{l=1}^{n_l} \delta(\mathbf{r} - \mathbf{r}_l(1/2)), \tag{1}$$

$$\hat{\Phi}_t(\mathbf{r}) = v_h \sum_{l=1}^{n_l} \int_0^1 \delta(\mathbf{r} - \mathbf{r}_l(s))\, ds, \tag{2}$$

$$\hat{\Phi}_s(\mathbf{r}) = v_h \sum_{j=1}^{n_s} \delta(\mathbf{r} - \mathbf{R}_{s,j}), \tag{3}$$

$$\hat{P}_h(\mathbf{r}) = -v_h \sum_{l=1}^{n_l} Q_{h,l}\delta(\mathbf{r} - \mathbf{r}_l(1/2)), \tag{4}$$

$$\hat{P}_c(\mathbf{r}) = v_h \sum_{i=1}^{n_c} \delta(\mathbf{r} - \mathbf{R}_{c,i}). \tag{5}$$

We have chosen v_h as a convenient volume to make all densities dimensionless. In the above, $\mathbf{R}_{s,j}$ is the position of the jth solvent particle, and $\mathbf{R}_{c,i}$ the position of the ith counter ion. The configuation of the lth lipid is described by a space curver $\mathbf{r}_l(s)$, where s ranges from 0 at the end of one tail, through $s = ½$ at which the head is located, to $s = 1$, the end of the other tail. The nominal probability that the charge on the headgroup of the lth lipid, $-eQ_{h,l}$, is equal to $-e$ or 0 is p or $1 - p$, respectively. As we model the case in which charges can associate or dissociate from the headgroup, it will be necessary to average the partition function of the system with respect to the charge distribution. This corresponds to an annealed distribution in the nomenclature of Borukhov et al. (1998). The concentrations of lipid, solvent, and free counter ions are controlled by chemical potentials. In particular, increasing the number of free, positive, counter ions implies, by charge neutrality, an increase in the negative charge on the headgroups, and thus corresponds to an increase in the pH of the system.

The interactions among these elements are as follows. First, there is a repulsive, contact interaction between headgroup and tail segments, and also between solvent and tail segments. The strength of the interaction is $kTv_h\chi$, where k is Boltzmann's constant and T the absolute temperature. Second, there is the Coulomb interaction between all charges. The dielectric constant of the solvent is denoted ϵ. Finally, there is a contact interaction between all charges and the neutral solvent, whose strength is $kTv_h\lambda$. This is to model the short-ranged, thermally averaged interaction between charges and the dipole of water, an attractive interaction that decreases like r^{-4} and is of strength $e^2u^2/6\epsilon^2kT$, where u is the dipole moment of water (Israelachvili, 1985). Thus, the energy per unit volume of the system, E/V, can be written

$$\begin{aligned}\frac{v_h}{kT}\frac{E}{V}[\hat{\Phi}_h, \hat{\Phi}_t, \hat{\Phi}_s, \hat{P}_h, \hat{P}_c] &= 2\chi N\int\frac{d\mathbf{r}}{V}[\hat{\Phi}_h(\mathbf{r}) + \hat{\Phi}_s(\mathbf{r})]\hat{\Phi}_t(\mathbf{r}) \\ &+ \frac{\beta^*}{8\pi}\int\frac{d\mathbf{r}}{V}\frac{d\mathbf{r}'}{R_g^2}[\hat{P}_h(\mathbf{r}) + \hat{P}_c(\mathbf{r})]\frac{1}{|\mathbf{r} - \mathbf{r}'|}[\hat{P}_h(\mathbf{r}') + \hat{P}_c(\mathbf{r}')] \\ &- \lambda\int\frac{d\mathbf{r}}{V}\hat{\Phi}_s(\mathbf{r})[\hat{P}_c(\mathbf{r}) - \hat{P}_h(\mathbf{r})],\end{aligned} \tag{6}$$

where

$$\beta^* \equiv \frac{4\pi e^2 R_g^2}{v_h\epsilon kT} \tag{7}$$

is a dimensionless measure of the strength of the Coulomb interaction. The grand partition function (Matsen, 1995) of the system is

$$\begin{aligned}\mathcal{Z} = \sum_{n_l,n_c,n_s}\frac{z_l^{n_l}z_c^{n_c}z_s^{n_s}}{n_l!\,n_c!\,n_s!}\int\prod_{l=1}^{n_l}\tilde{\mathcal{D}}\mathbf{r}_l\tilde{\mathcal{D}}Q_{h,l}\prod_{i=1}^{n_c}d\mathbf{R}_{c,i}\prod_{j=1}^{n_s}d\mathbf{R}_{s,j} \\ \times\exp\left\{-\frac{E[\hat{\Phi}_h, \hat{\Phi}_t, \hat{\Phi}_s, \hat{P}_h, \hat{P}_c]}{kT}\right\}\delta(1 - \hat{\Phi}_h - \gamma_s\hat{\Phi}_s \\ - \gamma_t\hat{\Phi}_t).\end{aligned} \tag{8}$$

Here, $\int\tilde{\mathcal{D}}\mathbf{r}_l$ denotes a functional integral over the possible configurations of the lth lipid and in which, in addition to the Boltzmann weight, the path is weighted by the factor $\mathcal{P}[\mathbf{r}_{t,l}(s); 0, 1]$, with

$$\mathcal{P}[\mathbf{r}, s_1, s_2] = \mathcal{N}\exp\left[-\frac{1}{8R_g^2}\int_{s_1}^{s_2}ds\left|\frac{d\mathbf{r}(s)}{ds}\right|^2\right], \tag{9}$$

with $\mathcal{N}$ an unimportant normalization constant. The notation $\int\tilde{\mathcal{D}}Q_{h,l}$ denotes an integral over the probability distribution of the charge on the headgroup of the lth lipid. We have enforced an incompressibility constraint on the system with the aid of the delta function $\delta(1 - \hat{\Phi}_h - \gamma_s\hat{\Phi}_s - \gamma_t\hat{\Phi}_t)$, where $\gamma_s = v_s/v_h$, and $\gamma_t = 2Nv_t/v_h$. The latter parameter is the lipid architectural parameter. The relative volume of the headgroup with respect to that of the entire molecule is $1/(1 + \gamma_t)$.

The model is now completely defined. The solvent is specified by γ_s, its volume per particle relative to that of the headgroup, and the architecture of the lipid is characterized by γ_t. There are three interactions, hydrophobic–hydrophilic, charge–charge, and charge–solvent, whose strengths are given by χ, β^*, and λ, respectively. The external parameters are the temperature, conveniently specified in terms of a dimensionless temperature $T^* \equiv (2\chi N)^{-1}$, the fugacity of the solvent, z_s, and the fugacity of the free counter ions, z_c, which, by charge neutrality, controls the charge on the lipid headgroups. The characteristic length in the system is the radius of gyration, R_g. In the next section, we derive the self-consistent field theory for the model, first in real space, and then in Fourier space.

THEORY

Real space

Evaluation of the partition function of Eq. 8 is difficult because the interactions are products of densities, each of

which depends on the specific coordinates of one of the elements of the system. This dependence is eliminated in a standard way. We illustrate it on $\hat{\Phi}_h(\mathbf{r})$ which, from its definition in Eq. 1, depends on the coordinates of the headgroup, $\mathbf{r}_l(½)$. One introduces into the partition function the identity

$$1 = \int \mathcal{D}\Phi_h \delta(\Phi_h - \hat{\Phi}_h),$$

$$= \int \mathcal{D}\Phi_h \mathcal{D}W_h \exp\left\{\frac{1}{v_h}\int W_h(\mathbf{r})[\Phi_h(\mathbf{r}) - \hat{\Phi}_h(\mathbf{r})]\,d\mathbf{r}\right\}, \tag{10}$$

in which $\Phi_h(\mathbf{r})$ does not depend on any specific coordinates of one of the elements of the system, but is simply a function of $\mathbf{r}$. The integration on W_h extends up the imaginary axis. Inserting such identities for the five densities $\hat{\Phi}_h$, $\hat{\Phi}_t$, $\hat{\Phi}_s$, $\hat{P}_h$, and $\hat{P}_c$, and a similar identity for the delta function expressing the incompressibility condition, one rewrites the partition function, Eq. 8, as

$$\begin{aligned}\mathcal{Z} = \int &\mathcal{D}\Phi_h \mathcal{D}W_h \mathcal{D}\Phi_t \mathcal{D}W_t \mathcal{D}\Phi_s \mathcal{D}W_s \mathcal{D}P_h \mathcal{D}U_h \mathcal{D}P_c \mathcal{D}U_c \mathcal{D}\Xi \\ &\times \exp\{z_l \mathcal{Q}_l[W_h, W_t, U_h] + z_c \mathcal{Q}_c[U_c] + z_s \mathcal{Q}_s[W_s] \\ &\quad - E[\Phi_h, \Phi_t, \Phi_s, P_h, P_c]/kT\} \\ &\times \exp\left\{\frac{1}{v_h}\int\left[W_h\Phi_h + W_t\Phi_t + W_s\Phi_s + U_hP_h + U_cP_c\right.\right. \\ &\quad \left.\left. + \Xi(1 - \Phi_h - \gamma_s\Phi_s - \gamma_t\Phi_t)\,d\mathbf{r}\right\},\end{aligned} \tag{11}$$

where

$$\begin{aligned}\mathcal{Q}_l[W_h, W_t, U_h] &= \int \tilde{\mathcal{D}}\mathbf{r}_l \tilde{\mathcal{D}} Q_h \exp\left\{-W_h\left(\mathbf{r}_l\left(\frac{1}{2}\right)\right) + Q_h U_h\left(\mathbf{r}_l\left(\frac{1}{2}\right)\right)\right. \\ &\quad \left. - \int_0^1 ds W_t(\mathbf{r}_l(s))\right\}\end{aligned} \tag{12}$$

is the partition function of a single lipid in external fields W_h, W_t, and U_h,

$$\mathcal{Q}_c[U_c] = \int d\mathbf{R}_c \exp[-U_c(\mathbf{R}_c)] \tag{13}$$

is the partition function of a single counter ion of unit positive charge in an external potential U_c, and

$$\mathcal{Q}_s[W_s] = \int d\mathbf{R}_s \exp[-W_s(\mathbf{R}_s)] \tag{14}$$

is the partition function of a single solvent particle in the external field W_s. It is convenient to shift the zero of all chemical potentials so that $z_l \to 1/v_h$, $z_c \to z_c/v_h$, and $z_s \to z_s/v_h$. The partition function, Eq. 11, can then be written in the form

$$\mathcal{Z} = \int \mathcal{D}\Phi_h \mathcal{D}W_h \mathcal{D}\Phi_t \mathcal{D}W_t \mathcal{D}\Phi_s \mathcal{D}W_s \mathcal{D}P_h \mathcal{D}U_h \mathcal{D}P_c \mathcal{D}U_c \mathcal{D}\Xi \exp\left[-\frac{\Omega}{kT}\right], \tag{15}$$

with

$$\begin{aligned}\frac{v_h}{kTV}\Omega = &-\frac{\mathcal{Q}_l[W_h, W_t, U_h]}{V} - z_c\frac{\mathcal{Q}_c[U_c]}{V} \\ &- z_s\frac{\mathcal{Q}_s[W_s]}{V} + \frac{v_h}{kTV}E[\Phi_h, \Phi_t, \Phi_s, P_h, P_c] \\ &- \int\frac{d\mathbf{r}}{V}[W_h\Phi_h + W_t\Phi_t + W_s\Phi_s + U_hP_h \\ &+ U_cP_c + \Xi(1 - \Phi_h - \gamma_s\Phi_s - \gamma_t\Phi_t)].\end{aligned} \tag{16}$$

No approximations have been made to this point. What has been accomplished is a rewriting of the partition function from a form, Eq. 8, in which all entities interact directly with one another, to a form, Eqs. 15 and 16, in which they interact indirectly with one another via fluctuating fields. Although the integrals in Eq. 15 over Φ_h, Φ_t, Φ_s, P_h, P_c, and Ξ could all be carried out, because they are no worse than Gaussian, the integrals over the fields W_h, W_t, W_s, U_h, and U_c cannot. Therefore, we use the self-consistent field theory in which we replace the integral in Eq. 15 by its integrand evaluated at its extremum. The values of W_h, Φ_h, etc., which satisfy the extremum conditions, will be denoted by the corresponding lower-case letters w_h, and ϕ_h, etc. The equations that determine them are six self-consistent equations for the six fields w_h, w_t, w_s, u_h, u_c, and ξ. They are

$$w_h(\mathbf{r}) = 2\chi N\phi_t(\mathbf{r}) + \xi(\mathbf{r}), \tag{17}$$

$$w_t(\mathbf{r}) = 2\chi N(\phi_h(\mathbf{r}) + \phi_s(\mathbf{r})) + \gamma_t\xi(\mathbf{r}), \tag{18}$$

$$w_s(\mathbf{r}) = 2\chi N\phi_t(\mathbf{r}) - \lambda(\rho_c(\mathbf{r}) - \rho_h(\mathbf{r})) + \gamma_s\xi(\mathbf{r}), \tag{19}$$

$$u(\mathbf{r}) \equiv \frac{u_h(\mathbf{r}) + u_c(\mathbf{r})}{2} = \frac{\beta^*}{4\pi}\int\frac{d\mathbf{r}'}{R_g^2}\frac{\rho_h(\mathbf{r}') + \rho_c(\mathbf{r}')}{|\mathbf{r} - \mathbf{r}'|}, \tag{20}$$

$$u_s(\mathbf{r}) \equiv \frac{u_h(\mathbf{r}) - u_c(\mathbf{r})}{2} = \lambda\phi_s(\mathbf{r}), \tag{21}$$

$$1 = \phi_h(\mathbf{r}) + \gamma_t\phi_t(\mathbf{r}) + \gamma_s\phi_s(\mathbf{r}). \tag{22}$$

Because the field ξ is easily eliminated, the six equations readily reduce to five. The simplicity of Eq. 21 reduces this, in practice, to a set of four equations. The five densities ϕ_h, ϕ_t, ϕ_s, ρ_h, and ρ_c are functionals of all of the above fields except ξ, and, therefore, close the cycle of self-consistent equations:

$$\phi_h(\mathbf{r})[w_h, w_t, u_h] = -\frac{\delta\mathcal{Q}_l[w_h, w_t, u_h]}{\delta w_h(\mathbf{r})}, \tag{23}$$

$$\phi_t(\mathbf{r})[w_h, w_t, u_h] = -\frac{\delta\mathcal{Q}_l[w_h, w_t, u_h]}{\delta w_t(\mathbf{r})}, \tag{24}$$

$$\phi_s(\mathbf{r})[w_s] = -z_s\frac{\delta\mathcal{Q}_s[w_s]}{\delta w_s(\mathbf{r})} \tag{25}$$

$$= z_s\exp[-w_s(\mathbf{r})], \tag{26}$$

$$\rho_h(\mathbf{r})[w_h, w_t, u_h] = -\frac{\delta\mathcal{Q}_l[w_h, w_t, u_h]}{\delta u_h(\mathbf{r})} \tag{27}$$

$$\rho_c(\mathbf{r})[u_c] = -\frac{\delta\mathcal{Q}_c[u_c]}{\delta u_c(\mathbf{r})} \tag{28}$$

$$= z_c\exp[-u_c(\mathbf{r})]. \tag{29}$$

The density $\phi_h(\mathbf{r})$ is simply the expectation value of $\hat{\Phi}_h(\mathbf{r})$ in the single lipid ensemble. Similar interpretations follow for the other densities. Note that one of the self-consistent equations, Eq. 20, is simply the nonlinear Poisson–Boltzmann equation, and $u(\mathbf{r})$ the electric potential.

With the aid of the above equations, the mean-field free energy, Ω_{mf}, which is the free energy function of Eq. 16 evaluated at the mean-field values of the densities and fields, can be put in the form

$$-\Omega_{mf} = \frac{kT}{v_h}(\mathcal{Q}_l[w_h, w_t, u_h] + z_c\mathcal{Q}_c[u_c] + z_s\mathcal{Q}_s[w_s]) + \mathrm{E}[\phi_h, \phi_t, \phi_s, \rho_h, \rho_c], \tag{30}$$

$$= kT(n_l + n_c + n_s) + \mathrm{E}[\phi_h, \phi_t, \phi_s, \rho_h, \rho_c] \tag{31}$$

with E given by Eq. 6. The thermodynamic potential, Ω, is that appropriate to an incompressible system calculated in the grand ensemble; the negative of the osmotic pressure multiplied by the volume. Thus, the above equation states that the osmotic pressure is the sum of the ideal partial osmotic pressures plus a correction due to the interactions. Within mean field theory, this correction is simply the energy per unit volume of the system.

We now specify that the charges in the system can associate with or disassociate from the headgroup in response to the local electrostatic potential. This implies that the partition function of a single lipid, $\mathcal{Q}_l$ is to be averaged over the nominal charge distribution that $Q_h = 1$ with probability p, and $Q_h = 0$ with probability $1 - p$ (Borukhov et al., 1998). The consequence of this averaging is that $\mathcal{Q}_l[w_h, w_t, u_h]$ of Eq. 12 becomes

$$\mathcal{Q}_l[w_{h,\mathrm{eff}}, w_t] = \int\tilde{\mathcal{D}}\mathbf{r}_l\exp\left\{-w_{h,\mathrm{eff}}\left(\mathbf{r}_l\left(\frac{1}{2}\right)\right) - \int_0^1 ds\, w_t(\mathbf{r}_l(s))\right\}, \tag{32}$$

where

$$w_{h,\mathrm{eff}}(\mathbf{r}) \equiv w_h(\mathbf{r}) - \ln\int\tilde{\mathcal{D}}Q_h\exp[Q_h u_h(\mathbf{r})] \tag{33}$$

$$= w_h(\mathbf{r}) - \ln[1 + p(\exp[u_h(\mathbf{r})] - 1)]. \tag{34}$$

Although this appears to introduce an unknown parameter p into the problem, the condition of charge neutrality,

$$\int d\mathbf{r}[\rho_h(\mathbf{r}) + \rho_c(\mathbf{r})] = 0, \tag{35}$$

relates this parameter to the fugacity of the counter ions, z_c. In practice, we use this fugacity to control the pH and the amount of charge on the lipids.

There remains only to specify how the single-lipid partition function is obtained. One defines the end-segment distribution function

$$q(\mathbf{r}, s) = \int\mathcal{D}\mathbf{r}_l(s)\delta(\mathbf{r} - \mathbf{r}_l(s))\exp\left\{-\int_0^s dt\left(\left[\frac{1}{8R_g^2}\left|\frac{d\mathbf{r}(t)}{dt}\right|^2\right] + w_{h,\mathrm{eff}}(\mathbf{r}_l(t))\delta\left(t - \frac{1}{2}\right) + w_t(\mathbf{r}_l(t))\right)\right\}, \tag{36}$$

which satisfies the equation

$$\frac{\partial q(\mathbf{r}, s)}{\partial s} = 2R_g^2\nabla^2 q(\mathbf{r}, s) - \left[w_{h,\mathrm{eff}}(\mathbf{r})\delta\left(s - \frac{1}{2}\right) + w_t(\mathbf{r})\right]q(\mathbf{r}, s), \tag{37}$$

with initial condition

$$q(\mathbf{r}, 0) = 1. \tag{38}$$

The partition function of the lipid is then

$$\mathcal{Q}_l = \int d\mathbf{r}\, q(\mathbf{r}, 1). \tag{39}$$

From this expression for the single-lipid partition function and Eqs. 23, 24, and 27, one obtains expressions for the local density of the lipid heads,

$$\phi_h(\mathbf{r}) = \exp[-w_{h,\mathrm{eff}}(\mathbf{r})]q\left(\mathbf{r}, \frac{1}{2} - \right)q\left(\mathbf{r}, \frac{1}{2} - \right), \quad (40)$$

of the lipid tails,

$$\phi_t(\mathbf{r}) = \int_0^1 \mathrm{d}s q(\mathbf{r}, s)q(\mathbf{r}, 1 - s), \quad (41)$$

and of the charge density on the lipid heads,

$$\rho_h(\mathbf{r}) = -\frac{p \exp[u_h(\mathbf{r})]}{1 + p(\exp[u_h(\mathbf{r})] - 1)} \phi_h(\mathbf{r}). \quad (42)$$

To summarize: there are four self-consistent equations to be solved for the fields w_h, w_t, w_s, and electrostatic potential u. These equations, obtained from simple algebraic manipulation of Eqs. 17–22, can be taken to be

$$\gamma_t w_h(\mathbf{r}) - w_t(\mathbf{r}) = 2\chi N[\gamma_t\phi_t(\mathbf{r}) - \phi_h(\mathbf{r}) - \phi_s(\mathbf{r})], \quad (43)$$

$$\gamma_s w_h(\mathbf{r}) - w_s(\mathbf{r}) = 2\chi N(\gamma_s - 1)\phi_t(\mathbf{r}) + \lambda(\rho_c(\mathbf{r}) - \rho_h(\mathbf{r})), \quad (44)$$

$$1 = \phi_h(\mathbf{r}) + \gamma_t\phi_t(\mathbf{r}) + \gamma_s\phi_s(\mathbf{r}), \quad (45)$$

$$R_g^2\nabla^2 u(\mathbf{r}) = -\beta^*(\rho_h(\mathbf{r}) + \rho_c(\mathbf{r})). \quad (46)$$

Note that we have chosen here to write the Poisson–Boltzmann equation, Eq. 20, in its local, rather than its integral form. When the four fields are known, the corresponding densities follow from Eqs. 26, 29, 40, 41, and 42.

Rather than attempt to solve these equations in real space, a difficult task for the periodic phases in which we are interested, such as H_{II}, we recast the equations in a form that makes straightforward their solution for a phase of arbitrary space–group symmetry (Matsen and Schick, 1994).

Fourier space

We note that the fields, densities, and the end point distribution function depend only on one coordinate $\mathbf{r}$. Therefore, in an ordered phase, these functions reflect the space–group symmetry of that phase. To make this symmetry manifest in the solution, we expand all functions of position in a complete, orthonormal set of functions, $f_i(\mathbf{r})$, $i = 1, 2, 3, \ldots$, each of which have the desired space group symmetry; e.g.,

$$\phi_h(\mathbf{r}) = \sum_i \phi_{h,i} f_i(\mathbf{r}), \quad (47)$$

$$\delta_{i,j} = \frac{1}{V}\int \mathrm{d}\mathbf{r} f_i(\mathbf{r}) f_j(\mathbf{r}). \quad (48)$$

Furthermore, we choose the $f_i(\mathbf{r})$ to be eigenfunctions of the Laplacian

$$\nabla^2 f_i(\mathbf{r}) = -\frac{\lambda_i}{D^2} f_i(\mathbf{r}), \quad (49)$$

where D is a length scale for the phase. The functions for the lamellar phase are clear. They can be taken to be

$$f_1(\mathbf{r}) = 1, \quad (50)$$

$$f_i(\mathbf{r}) = \sqrt{2}\cos[2\pi(i-1)x/D] \quad i \geq 2. \quad (51)$$

Expressions for the unnormalized basis functions for other space–group symmetries can be found in X-ray tables (Henry and Lonsdale, 1969) because they are intimately related to the Bragg peaks. In the tables cited, those for the hexagonal phase, space group (p6m) can be found on page 372, and that of the bcc phase, space group (Im3m) on page 524.

The four self-consistent equations become

$$\gamma_t w_{h,i} - w_{t,i} = 2\chi N[\gamma_t\phi_{t;i} - \phi_{h;i} - \phi_{s;i}], \quad (52)$$

$$\gamma_s w_{h;i} - w_{s;i} = 2\chi N(\gamma_s - 1)\phi_{t;i} + \lambda(\rho_{c;i} - \rho_{h;i}), \quad (53)$$

$$\delta_{1,i} = \phi_{h;i} + \gamma_t\phi_{t;i} + \gamma_s\phi_{s;i}, \quad (54)$$

$$\frac{\lambda_i R_g^2}{D^2} u_i = \beta^*(\rho_{h;i} + \rho_{c;i}). \quad (55)$$

To obtain the partition functions and densities, we proceed as follows. For any function $G(\mathbf{r})$, we can define a symmetric matrix,

$$(G)_{ij} \equiv \frac{1}{V}\int f_i(\mathbf{r})G(\mathbf{r})f_j(\mathbf{r})\,\mathrm{d}\mathbf{r}. \quad (56)$$

Note that $(G)_{1i} = (G)_{i1} = G_i$, the coefficient of $f_i(\mathbf{r})$ in the expansion of $G(\mathbf{r})$. Matrices corresponding to functions of $G(\mathbf{r})$, such as

$$(e^G)_{ij} \equiv \frac{1}{V}\int f_i(\mathbf{r})e^{G(\mathbf{r})}f_j(\mathbf{r})\,\mathrm{d}\mathbf{r}, \quad (57)$$

are evaluated by making an orthogonal transformation, which diagonalizes $(G)_{ij}$. With this definition, Eqs. 26 and 29 yield the solvent density and counter ion charge density,

$$\phi_{s;i} = z_s(e^{-w_s})_{i,1}, \quad (58)$$

$$\rho_{c;i} = z_c(e^{-u_c})_{i,1} \quad (59)$$

$$= z_c(e^{-(u-u_s)})_{i,1}. \quad (60)$$

To obtain the remaining densities, we need the end-point distribution function. From Eq. 37, we obtain

$$\frac{\mathrm{d}q_i(s)}{\mathrm{d}s} = -\sum_j [A_{ij} + (w_{h,eff})_{ij}\delta(s - 1/2)]q_j(s), \quad (61)$$

$$A_{ij} = \frac{2R_g^2}{D^2}\lambda_i\delta_{ij} + (w_t)_{ij}, \quad (62)$$

with initial condition $q_i(0) = \delta_{i,1}$. The solution of this equation is

$$\begin{aligned} q_i(s) &= (e^{-As})_{i,1} \quad \text{if } s < \tfrac{1}{2}, \\ &= \sum_j (e^{-w_{h,eff}})_{ij}(e^{-A/2})_{j,1} \quad s = \tfrac{1}{2}, \\ &= \sum_{j,k} (e^{-A(s-1/2)})_{i,j}(e^{-w_{h,eff}})_{jk}(e^{-A/2})_{k,1} \quad s > \tfrac{1}{2}. \end{aligned} \quad (63)$$

From this, the remaining densities follow from Eqs. 40, 41, and 42:

$$\phi_{h;i} = \sum_{jkl} (e^{-w_{h,eff}})_{ij}\Gamma_{jkl}q_k(\tfrac{1}{2}-)q_l(\tfrac{1}{2}-), \quad (64)$$

$$\phi_{t;i} = \int_0^1 \mathrm{d}s \sum_{jk} \Gamma_{ijk}q_j(s)q_k(1-s), \quad (65)$$

$$\rho_{h;i} = -\sum_j \left(\frac{pe^{u_h}}{1 + p(e^{u_h} - 1)}\right)_{i,j} \phi_{h;j}, \quad (66)$$

with

$$\Gamma_{ijk} \equiv \frac{1}{V}\int f_i(\mathbf{r})f_j(\mathbf{r})f_k(\mathbf{r})\, d\mathbf{r}. \quad (67)$$

The mean-field free energy, Eq. 31, takes the form

$$-\Omega_{mf} = \frac{kTV}{v_h}(\phi_{t;1} + \phi_{s;1} + \rho_{c;1}) + E, \quad (68)$$

with the mean-field energy being given by

$$E = \frac{kTV}{v_h}\sum_i [2\chi N(\phi_{h;i} + \phi_{s;i})\phi_{t;i} + \tfrac{1}{2}(\rho_{h;i} + \rho_{c;i})u_i - \lambda(\rho_{c;i} - \rho_{h;i})\phi_{s;i}]. \quad (69)$$

We have expressed the Coulomb energy as a product of the charge densities and electrostatic potential. Note that this free energy still depends parametrically on D, the length scale of the phase, so that the value of D that minimizes it must be determined. Once this is done, we compare the free energies obtained for phases of different space–group symmetry, and thereby determine the phase diagram of our model lipid system.

The infinite set of self-consistent equations, Eqs. 52–55 must be truncated to be solved numerically. We have used up to 50 basis functions. This truncation is sufficient to ensure, for $T^* > 0.03$ and $1/(1 + \gamma_t) < 0.66$, an accuracy of 10^{-4} in the free energy $v_h\Omega_{mf}/kTV$. As noted, one must also determine the length scale that minimizes the free energy. This is usually straightforward because there is a single well-defined minimum for a phase of given symmetry at given thermodynamic parameters: temperature, and chemical potentials. Were there more than one minimum, this would reflect a tendency for the system to phase separate into two phases with the same nontrivial space–group symmetry, an extremely unusual occurrence. The single minimum that one finds normally is sharp, that is, the free energy varies rather rapidly with D. Only in cases in which phases are greatly swollen is the minimum extremely shallow and difficult to locate.

RESULTS

The neutral lipid

We first apply our method to a neutral lipid. We show here the phase behavior of the neutral lipid, in the absence and in the presence of solvent. Figure 1 shows the phase diagram of the pure lipid as a function of the dimensionless temperature T^*, and the architecture of the lipid. The latter is characterized by the single parameter $1/(1 + \gamma_t)$ which is

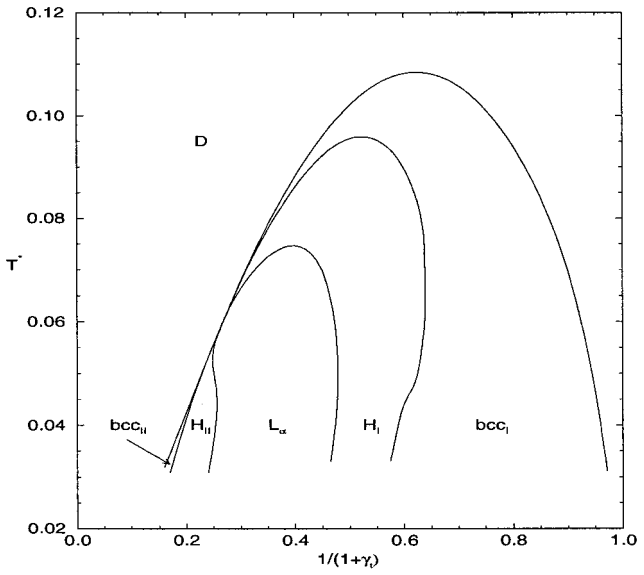

FIGURE 1 Phase diagram of the neutral lipid as a function of dimensionless temperature, $T^* \equiv 1/2\chi N$, and relative headgroup volume, $1/(1 + \gamma_t)$. In addition to the disordered phase, D, there are normal and inverted body-centered cubic phases, bcc_I and bcc_{II}, normal and inverted hexagonal phases, H_I and H_{II}, and the lamellar phase L_α.

the relative volume of the headgroup to that of the entire lipid. It is analogous to, but not the same as, the single parameter used by Israelachvili (1985) to characterize the geometry of lipids. Shown are the lamellar phase, L_α, the normal and inverted hexagonal phases, H_I and H_{II}, and the normal and inverted body-centered cubic phases bcc_I and bcc_{II}. The occurrence of bicontinuous phases will be discussed in a later paper.

One sees that the phase behavior is reasonable and in accord with packing considerations; as the headgroup increases in volume, the system passes through a series of phases from the inverted ones with most curvature, through the lamellar phase, to the normal ones of most curvature. To model a lipid, which, like phosphatidylserine, adopts the H_{II} configuration when essentially neutral (Cullis et al., 1985, Bezrukov et al., 1998), we have chosen $1/(1 + \gamma_t) = 0.24$ in our subsequent studies. For comparison, the value appropriate for DOPE, calculated from the molecular volumes in the literature (Rand and Fuller, 1994), is 0.254. For the convenience of the reader interested in carrying out similar calculations, we present, in Table 1, the values of the first three nontrivial Fourier components of the headgroup density $\phi_h(\mathbf{r})$, the lattice parameter D/R_g, and the free energy $\Omega_{mf}\nu_h/kTV$ for the L_α, H_{II}, and bcc_{II} phases at $T^* = 0.04$. We note, in passing, that the relative intensities of X-ray Bragg peaks can be determined directly from the Fourier components of the various densities with which they are associated.

The effect on this neutral lipid of the addition of a solvent of small volume, characterized by $\gamma_s = \nu_s/\nu_h = 0.1$, close to the value of 0.096 (Rand and Fuller, 1994; Kozlov et al., 1994), appropriate to water and a phosphatidylethanolamine headgroup, is shown in Fig. 2. There is a lamellar phase at small solvent volume fractions and low temperatures. This phase becomes unstable with respect to the H_{II} phase, which envelops it at higher temperatures. There is a large region of two-phase coexistence between the ordered lipid-rich phases and an almost pure solvent phase. These features are reasonable, and are observed in the systems of aqueous dialkyl didodecylphosphatidylethanolamine and of diacyl diarachinoylphosphatidylethanolamine (Seddon et al., 1984). Of particular interest is that we find a small temperature region of re-entrant hexagonal-lamellar-hexagonal transitions, an unusual feature that has been observed in

TABLE 1 Anhydrous, neutral lipid: the lattice parameter, the free energy, and the first three non-trivial Fourier components of $\phi_h(r)$ for L_α, H_{II}, and bcc_{II} phases at $T^* = 0.04$ and $1/(1 + \gamma_t) = 0.24$

	D/R_g	$\nu_h\Omega_{mf}/kTV$	$\phi_{h,2}$	$\phi_{h,3} \times 10^2$	$\phi_{h,4} \times 10^2$
L_α	2.921	0.7969	0.2272	6.781	−1.171
H_{II}	3.167	0.7936	0.2368	0.476	−2.372
bcc_{II}	3.400	0.8027	0.2204	1.094	−4.038

Note that $\phi_{h,1} = \phi_{t,1} = 0.24$ for all phases.

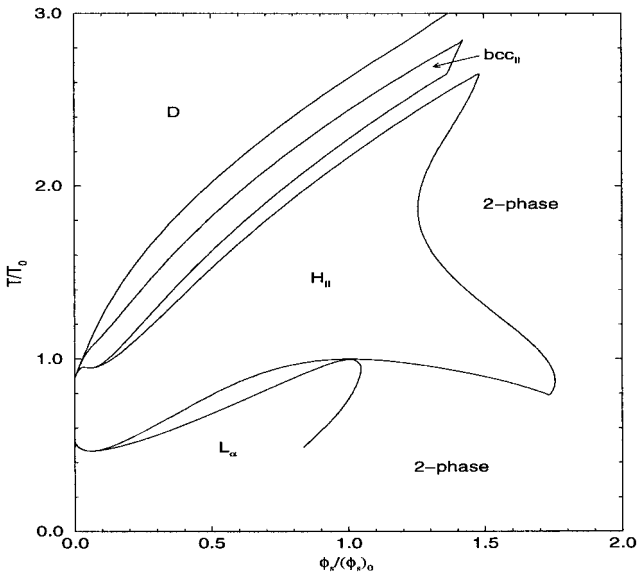

FIGURE 2 Phase diagram of a neutral lipid with $1/(1 + \gamma_t) = 0.24$ in a solvent with $\gamma_s = 0.1$ as a function of temperature, T/T_0, and fraction of solvent, $\phi_s/(\phi_s)_0$, with T_0 and $\gamma_s(\phi_s)_0$ the temperature and volume fraction of solvent at the azeotrope.

DOPE (Gawrisch et al. 1992; Kozlov et al. 1994). As a consequence, there is an azeotrope at which the transition between lamellar and hexagonal phases occurs without a change in the concentration of water. We have used the coordinates of this point, $T^* = 0.06$ and $\phi_s = 1.42$, denoted T_0 and $(\phi_s)_0$, to normalize the temperature and solvent–density axes. There is a small region of bcc_{II} in our phase diagram. Again, the possible occurrence of bicontinuous phases will be examined in a later publication. The uncertainty in the temperature of the phase boundaries, $\delta T/T$ introduced by the truncation of the number of basis functions, is approximately 2×10^{-3}.

As the volume fraction of water is increased, we find that the period of all structures increases, as is expected. In Fig. 3, we compare experimental results on DOPE taken in the inverted hexagonal phase at a temperature $T = 22°C$, just above that of the azeotrope (Rand and Fuller, 1994), to our values calculated just above the azeotrope. Knowing the molecular weight of DOPE, we convert the volume fraction of solvent, $\gamma_s\phi_s$, which occurs in the calculation, to the experimental variable of weight fraction of water. The lattice parameter of the hexagonal phase in the calculation, however, is measured in units of the radius of gyration of either lipid tail. What value should be taken to model DOPE is unknown. Hence, we have used, in the comparison, the lattice parameter D, in units of D_0, the lattice parameter at the azeotrope. The agreement is excellent.

An effective value of the radius of gyration can be defined as that value that brings agreement between the calculated and measured lattice parameters. As the former, at the azeotrope, is $D(T_0) \equiv D_0 = 4.79R_g^0$, and the latter is 58.9

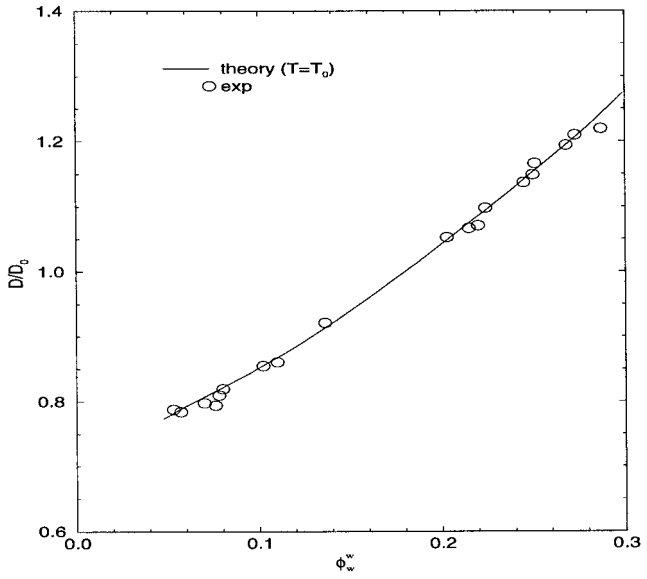

FIGURE 3 Comparison of theoretically calculated and experimentally measured values of the lattice parameter D/D_0 of the H_{II} phase at a temperature just above the azeotrope versus weight fraction of water, ϕ_w^w. The lattice parameter at the azeotrope is denoted D_0.

Å (Rand and Fuller, 1994), the equivalent radius of gyration at the temperature of the azeotrope, R_g^0, is 12.3 Å for a single tail, not unreasonable when compared to the extended length of a single chain of DOPE, which is approximately 26 Å.

As the temperature of the system is lowered, the period of all structures increases, which is due to the lengthening of the tails as their entropy decreases. We would again like to compare our results with those of the DOPE system. To do so, we must address the temperature dependence of the radius of gyration, R_g, which appears in the theory, and which is not given a priori. Because the model chain is flexible, the radius of gyration is related to the mean square end-to-end distance, $\bar{R}$, by a numerical constant, $R_g = \bar{R}/\sqrt{6}$, so their dependence on temperature is the same. To compare our results to DOPE, we shall assume that the temperature dependence of the radius of gyration that appears in the calculation is the same as that given for lipid chains by the Rotational Isomeric States Model, a model that describes the properties of such chains very well (Flory, 1969; Mattice and Suter, 1994). Thus we assume

$$R_g(T) = c\left(\frac{1 - \langle\cos\phi\rangle}{1 + \langle\cos\phi\rangle}\right)^{1/2}, \tag{70}$$

where the angle ϕ takes the values 180° and ±70° corresponding to trans, gauche$^+$ and gauche$^-$ configurations, and c is a constant. The statistical average of cos ϕ is

$$\langle\cos\phi\rangle = \frac{\cos(180°) + \sigma\cos(70°) + \sigma\cos(-70°)}{1 + 2\sigma}, \tag{71}$$

with $\sigma = \exp(-T_{rism}/T)$ and $T_{rism} = 280.25$ K. From the behavior with temperature of $R_g(T)$, the lattice parameter, $D(T)$, at any temperature can be obtained from

$$\frac{D(T)}{D(T_0)} = \frac{[D(T)/R_g(T)]}{[D(T_0)/R_g(T_0)]}\frac{R_g(T)}{R_g(T_0)}, \tag{72}$$

Again, it is the factor $D(T)/R_g(T)$ that occurs naturally in the calculation.

A comparison of the experimentally measured (Kirk and Grunner, 1985; Tate and Gruner, 1989) and theoretically calculated lattice parameters versus temperature is shown in Fig. 4. In part (*a*), the variation of the parameter of the H_{II} is shown at two different lipid weight fractions. The agreement is very good. In part (*b*), the comparison is made of the H_{II} and L_α parameters along the coexistence with excess water. Note that this comparison is a much more stringent test, because it requires not only that the dependence of the lattice parameters on solvent concentration and on temperature be reproduced well by the calculation, but also that the phase boundaries be given well. Considering these requirements, the agreement is rather good. It should be noted that the agreement in Fig. 4 *b* does not depend on the exact temperature of the triple point, which is difficult to locate precisely, but only on the existence of stable H_{II} and L_α phases, which coexist with excess water.

As seen in Fig. 4 *b*, the lattice parameter of the H_{II} phase is much larger than that of the L_α at the triple point. This is due to the coexistence with excess solvent, which swells the

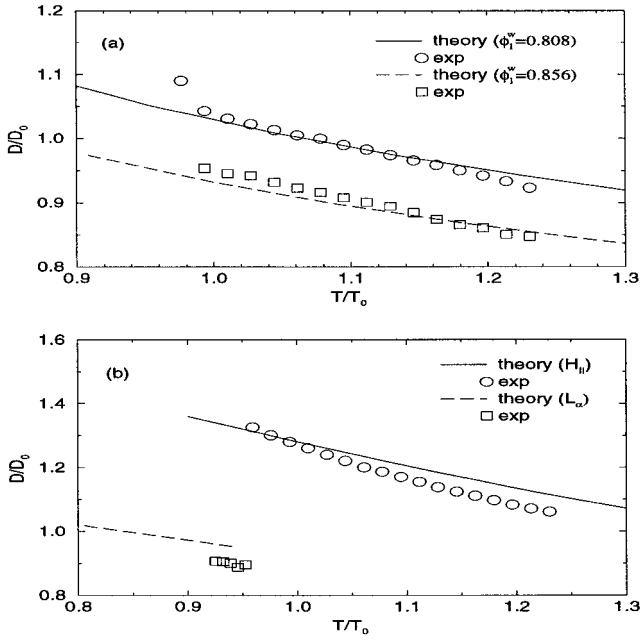

FIGURE 4 Comparison of theoretically calculated and experimentally measured values of the lattice parameter, $D(T)/D_0$, versus absolute temperature T (*a*) for two different weight fractions of lipid, ϕ_1^w, and (*b*) along coexistence with excess water. The absolute temperature of the azeotrope is denoted T_0.

hexagonal cores, but which is only weakly present between the lamellae. In contrast, when the lamellar and hexagonal phases are only in two-phase coexistence with one another and there is no excess solvent, the hexagonal phase, in general, has a smaller lattice parameter than the coexisting lamellar phase, as shown in Fig. 5. This is because, over almost all of their coexistence region, the H_{II} phase has a smaller volume fraction of solvent than does the L_α phase, as can be seen from the phase diagram of Fig. 2. Only over the re-entrant region, which occurs as the triple point is approached, does this balance shift. This shift in the relative size of the latter parameters through the re-entrant region is in agreement with experiment (Kozlov et al., 1994).

It is of interest to determine if any one effect can be said to drive the transition from the H_{II} to L_α phase in the neutral system. To this end, we examine the individual terms in the thermodynamic potentials per unit volume $\Omega_{mf}v_h/kTV = Ev_h/kTV - S_lv_h/kV - (S_sv_h/kV + \phi_s\ln z_s)$ of the L_α and H_{II} phases, as the transition is crossed, by increasing the solvent fugacity, z_s, at constant temperature $T/T_0 = 0.67$. In Table 2, we show the contributions to the free energy per unit volume of the L_α phase and that of the H_{II} phase coming from the interaction energy, Ev_h/kTV, the lipid tails, $-S_lv_h/kV$, and the solvent $-S_sv_h/kV - \phi_s\ln z_s$. All contributions are evaluated at the transition itself, which occurs at $z_s \approx 3.15$, and are measured with respect to the free energy per unit volume of the disordered phase. We also show the difference in the contribution of each term to the free energies of each phase, and the derivative of this difference with respect to the solvent fugacity. The difference in the contribution of the entropy of the lipid tails is positive because, with the lipid architecture we have chosen, the large tail volume relative to that of the head favors the hexagonal phase. The interaction energy favors the lamellar phase, as does the solvent, presumably because the interstices of that phase are two-dimensional, whereas those of the inverted hexagonal phase are one-dimensional. The difference between the lipid entropy contributions decreases with increasing solvent concentration because the packing constraints in the H_{II} phase become more severe as the size of the cores increases (Gruner, 1989). However, it is apparent that neither this term, nor either of the others, changes so rapidly with solvent concentration compared to the others that any particular effect can be said to drive this transition.

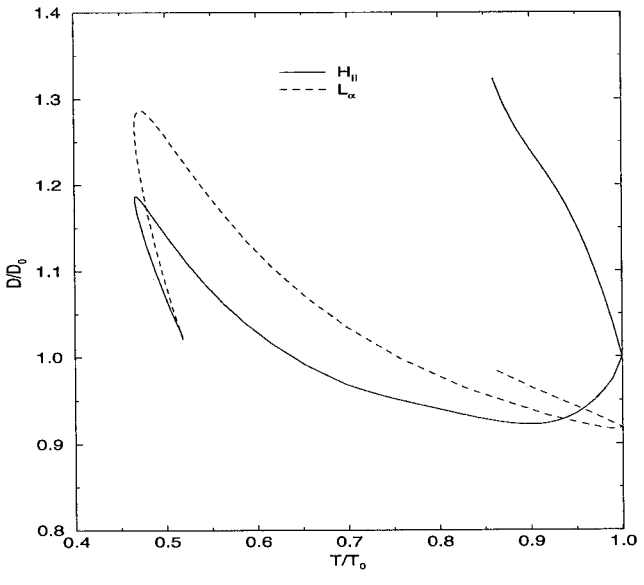

FIGURE 5 Lattice parameter of the H_{II} and L_α phases along their mutual coexistence as a function of absolute temperature. The absolute temperature of the azeotrope is denoted T_0.

TABLE 2 Neutral lipid: contributions to the free energy per unit volume and temperature in the L_α phase and in the H_{II} phase, the difference in these contributions, and the derivative of this difference with respect to the solvent fugacity

	$L_\alpha - D$	$H_{II} - D$	$L_\alpha - H_{II}$	$d(L_\alpha - H_{II})/dz_s$
$\mathscr{E}$	−0.6923	−0.6086	−0.0837	0.0244
$-\mathscr{S}_l$	1.1367	0.9123	0.2250	−0.0413
$-\mathscr{S}_s$	−0.6666	−0.5253	−0.1413	−0.0394

All contributions are evaluated at the L_α, H_{II} transition occurring on the water-poor side of the azeotrope. The solvent chemical potential at the transition is $z_s \approx 3.15$. All contributions are measured with respect to the free energy of the disordered phase, (D). The temperature, $T/T_0 = 0.67$. $\mathscr{E} \equiv v_hE/VkT$, $\mathscr{S}_l \equiv v_hS_l/Vk$, and $\mathscr{S}_s \equiv v_hS_s/Vk + \phi_s\ln z_s$.

The charged lipid

We now turn on the negative charge of the headgroups by varying the chemical potential of the free counter ions while enforcing charge neutrality. Increasing the density of free, positive counter ions in our closed system is equivalent to increasing the magnitude of the negative charge density on the headgroups. It therefore corresponds to an increase in the pH of an experimental system. The charge on the headgroups is annealed, meaning that it is determined by the local value of the electrostatic potential, and therefore the headgroup charge varies with the location of that group. The parameter β^*, defined in Eq. 7, measures the strength of the Coulomb interaction. It can be written as the ratio of two lengths, $\beta^* = \xi/L_l$, where $\xi \equiv e^2/\epsilon kT$ is the Bjerrum length, and $L_l \equiv v_h/4\pi R_G^2$ is a length characterizing the architecture of the lipid. It is reasonable that β^* be larger than, or of order, unity, and we have arbitrarily taken $\beta^* = 1$.

In addition to the Coulomb interaction, the short-ranged, thermally averaged interaction between charges and the water dipole is also of importance. It varies with separation r as $(kT/6)(u/e\xi)^2(\xi/r)^4 \equiv \omega(r)$, with u the dipole moment of water and ξ the Bjerrum length. The above expression is valid for distances such that $r/\xi > (u/e\xi)^{1/2}$. For water, $\xi \approx 7$ Å, and $\omega(r)/kT \approx 4.6 \times 10^{-4}(\xi/r)^4$. To approximate this short-ranged interaction by a contact interaction of dimensionless strength, λ, is equivalent to using ω/kT evaluated at

some fixed distance. Any reasonable choice shows that λ is small. We have arbitrarily chosen $\lambda = 0.1$, which corresponds to $\omega(r)/kT$ evaluated at 1.9 Å, a distance within the regime in which the approximate expression for the charge–dipole interaction is valid.

Shown in Fig. 6 is the temperature of the transition, T^*, between H_{II} and L_α phases as a function of the magnitude of the average charge density on the headgroups, $\bar{\rho}_h \equiv \rho_{h;1}$. The range of charge density corresponds to the headgroups varying from being neutral to fully charged. The region beyond the almost vertical line at $|\bar{\rho}_h| \approx 0.22$ would correspond to the headgroups being charged with a probability greater than unity, and is therefore unphysical. The maximum value of $|\bar{\rho}_h|$ is slightly different in the two phases. One sees that, with increasing headgroup charge equivalent to increasing pH, the inverted hexagonal phase becomes unstable with respect to the lamellar phase, just as in the experiments on phosphatidylserine in water (Hope and Cullis, 1980; Bezrukov et al., 1998). Furthermore, the pH at the transition increases with increasing temperature, in accord with experiment (Hope and Cullis, 1980).

In Fig. 7 *a*, we show the volume fraction profiles in the L_α phase at a value of $z_c = 0.1228$, $z_s = 3$, and temperature $T^* = 0.04$ at which the $H_{II} - L_\alpha$ transition occurs. The position through the system is divided by the lattice parameter of the phase, which, in units of the radius of gyration of the lipid, is $D_L/R_g \approx 4.14$. All looks reasonable. In particular, the volume fraction of solvent within the bilayer is negligible, in agreement with molecular dynamic simulations of a single charged bilayer (López Cascales et al., 1996). We obtain similar results when the lipid is neutral. In Fig. 7 *b*, the charge density profile of the same structure is shown. One sees that the charge on the headgroup mimics, but does not reproduce, the headgroup volume fraction. This is because the charge on the headgroup is not fixed, but varies with the local electrostatic potential. The counter ion density is fairly uniform because we have used a single dielectric constant, that of water, throughout the system. In principle, a more realistic position-dependent dielectric constant could be used, which would lead to a reduced counter ion density in the tail region. Such a procedure would entail a significant change in the Poisson–Boltzmann equation, Eq. 46, because it is the divergence of the electric displacement.

$$-\nabla \cdot [\epsilon(\mathbf{r})\nabla u(\mathbf{r})] = -\epsilon(\mathbf{r})\nabla^2 u(\mathbf{r}) - \nabla u(\mathbf{r}) \cdot \nabla \epsilon(\mathbf{r}), \qquad (73)$$

that is proportional to the free charge density. The second term cannot be ignored in the region around the headgroups where the dielectric constant varies rapidly between its values in the tail and water regions. It accounts for the orientation of water dipoles near the headgroups. The fact that the position-dependent dielectric constant depends on the initially unknown head, tail, and solvent densities, $\epsilon(\mathbf{r}) = \epsilon_h\hat{\Phi}_h(\mathbf{r}) + \epsilon_t\gamma_t\hat{\Phi}_t(\mathbf{r}) + \epsilon_s\gamma_s\Phi_s(\mathbf{r})$, further complicates the equation. For these reasons, we have used the uniform dielectric constant in this initial study. Interestingly, the approximation of a uniform dielectric would have much less effect had we modeled larger counter ions, such as Na^+. Their very size, coupled with the incompressibility condi-

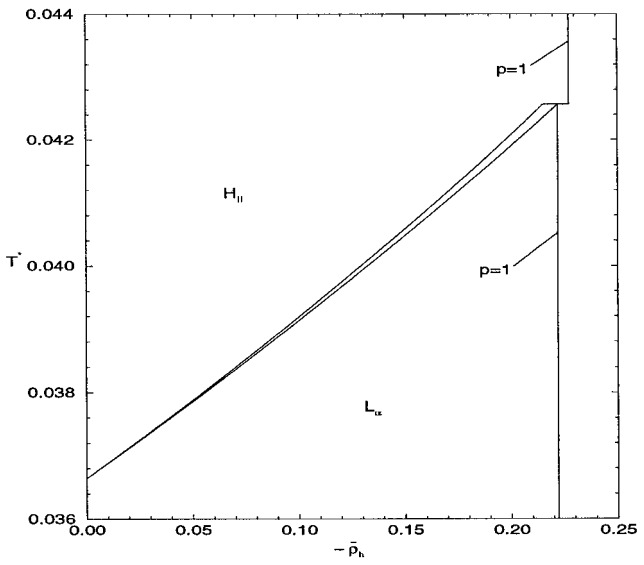

FIGURE 6 Transition temperature between L_α and H_{II} phases for the same lipid as in Fig. 2, but now with a charged headgroup. The dimensionless strength of the Coulomb interaction is $\beta^* = 1$, and that of the interaction between charges and neutral solvent is $\lambda = 0.1$. The solvent fugacity is fixed at $z_s = 3$.

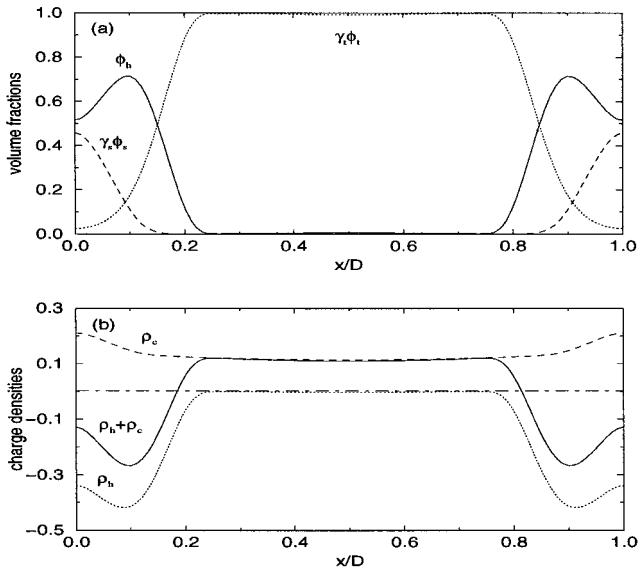

FIGURE 7 (*a*) Volume fraction distribution in the L_α phase of the solvent, headgroups, and tails, in the system of Fig. 6 at a counter ion chemical potential of $z_c = 0.1228$ corresponding to the $L_\alpha - H_{II}$ transition. The temperature is $T^* = 0.04$, and the lattice parameter of the lamellar phase is $D_L/R_g = 4.14$. (*b*) Charge densities arising from the headgroups, the counter ions, and the total charge density in the L_α phase under the same conditions as in (*a*).

tions and the interactions, would cause their density in the tail region to be much reduced (López Cascales et al., 1996) when calculated by the Poisson–Boltzmann equation (Borukhov et al., 1997).

In Fig. 8 *a* and *b*, we show the volume fraction and charge density profiles for the H_{II} phase at the same value of z_c as in Fig. 7. The cut through the system is taken along the nearest-neighbor direction, and the distance is normalized to its lattice parameter $D_H \approx 3.83R_g$. Again, the wavelength of the H_{II} phase is smaller than that of the L_α phase because, in two-phase coexistence, i.e., in the absence of a reservoir of excess water, the cores of the cylinders are not swollen with water, and the hexagonal phase contains a smaller volume fraction of water than does the lamellar phase. One can infer from Fig. 8 *a* that, in the nearest-neighbor direction, there is far more interdigitation of lipid tails than in the lamellar phase. This makes sense, because the tails must certainly stretch to fill the space between cores in the second-neighbor direction, so that interdigitation is expected in the nearest-neighbor direction.

To investigate this transition further, we show, in Table 3, the contributions in the L_α and the H_{II} phases of the various terms in the thermodynamic potential per unit volume $\Omega_{mf}v_h/kTV = (E_1 + E_2 + E_3)v_h/kTV - S_lv_h/kV - (S_sv_h/kV + \phi_s \ln z_s) - (S_cv_h/kV + \rho_c \ln z_c)$. Here E_1 is the hydrophilic–hydrophobic interaction proportional to χN, E_2 is the electrostatic interaction proportional to β^*, and E_3 is the charge–solvent interaction proportional to λ. These contributions are evaluated at the transition itself, and are measured from the free energy per unit volume of the disordered phase. We also show the difference between these contributions to each phase, and the derivatives of each of these differences with respect to the counter ion fugacity, z_c. There are several interesting things to note. The electrostatic energy is a relatively small contribution to the free energy of each phase, and hardly differs between them. Therefore, it does not have a large effect in bringing about the transition. The contribution of the counter ions to the free energy of each phase is of the same order of magnitude as the electrostatic interaction and, like it, does not change rapidly with the counter ion fugacity. The contribution of the short-range charge–solvent interaction is small, but it changes most rapidly with the counter ion fugacity, and, therefore, appears to be most important in actually bringing about the transition itself.

TABLE 3 Charged lipid with both Coulomb and charge–solvent interactions: contributions to the free energy per unit volume and temperature in the L_α the H_{II} phases, the difference in these contributions, and the derivative of this difference with respect to the counter ion fugacity

	$L_\alpha - D$	$H_{II} - D$	$L_\alpha - H_{II}$	$d(L_\alpha - H_{II})/dz_c$
$\mathscr{E}_1$	−0.6904	−0.6059	−0.0845	0.0152
$\mathscr{E}_2$	0.0037	0.0024	0.0013	0.0196
$\mathscr{E}_3$	−0.0378	−0.0268	−0.0110	−0.1082
$-\mathscr{S}_l$	1.1373	0.9110	0.2263	−0.0257
$-\mathscr{S}_s$	−0.6365	−0.5034	−0.1331	0.0215
$-\mathscr{S}_c$	0.0030	0.0020	0.0010	0.0153

All contributions are evaluated at the L_α, H_{II} transition, $z_c = 0.1228$, and are measured with respect to the free energy of the disordered phase, (D). The temperature, $T^* = 0.04$, $z_s = 3$, $\mathscr{E}_i \equiv v_hE_i/VkT$, with $i = 1, 2, 3$ being the hydrophilic–hydrophobic, Coulomb, and charge–neutral interactions, respectively, $\mathscr{S}_l \equiv v_hS_l/Vk$, $\mathscr{S}_s \equiv v_hS_s/Vk + \phi_s \ln z_s$, and $\mathscr{S}_c \equiv v_hS_c/Vk + \rho_c \ln z_c$.

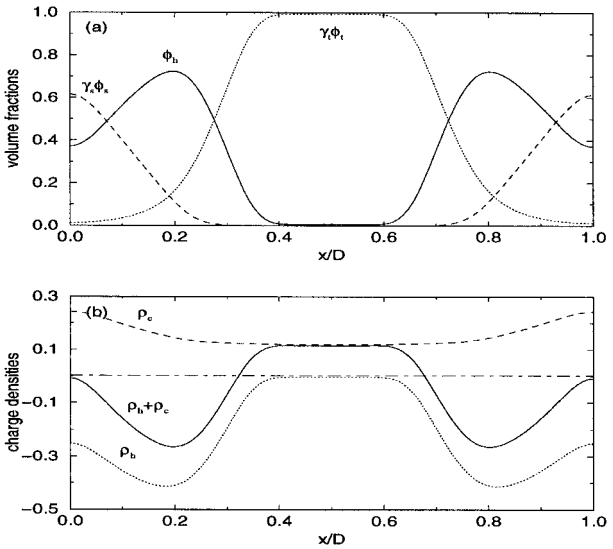

FIGURE 8 (*a*) Volume fraction distribution in the H_{II} phase of the solvent, headgroups, and tails, in the system of Fig. 6 at a counter ion chemical potential of $z_c = 0.1228$ corresponding to the $L_\alpha - H_{II}$ transition. The temperature is $T^* = 0.04$, and the lattice parameter of the inverted hexagonal phase is $D_H/R_g = 3.83$. (*b*) Charge densities arising from the headgroups, the counter ions, and the total charge density in the H_{II} phase under the same conditions as in (*a*).

The physical mechanism in the experimental system appears to be clear. The lipid with an almost neutral headgroup forms the H_{II} phase because the volume of the headgroup is relatively small compared to that of the entire lipid. As the charge on the headgroup is turned on, it attracts an increasing volume of waters of hydration via the attractive interaction between the charge and the dipoles of water. In addition, more counter ions, enlarged by their own waters of hydration, are attracted to the headgroup. Thus, the headgroup becomes effectively larger, and drives the transition to the L_α phase.

Just as we have calculated the variation with temperature and solvent concentration of the H_{II} lattice constant of neutral DOPE, so we should be able to calculate its recently measured variation with salt concentration in binary mixtures of DOPE and dioleoylphosphatidic acid, (Döbereiner, unpublished). It would be interesting to do so.

We gratefully acknowledge useful communications with Drs. Pieter Cullis, John Seddon, and Sol Gruner.

This work was supported in part by the National Science Foundation under grant numbers DMR9531161 and DMR9876864. M. S. would like to thank the Commissariat à l'énergie atomique, Saclay, for their gracious hospitality while this paper was being written.

REFERENCES

Ben-Shaul, A., I. Szleifer, and W. M. Gelbart. 1985. Chain organization and thermodynamics in micelles and bilayers. I. Theory. *J. Chem. Phys.* 83:3597–3611.

Bezrukov, S. M., R. P. Rand, I. Vodyanoy, and V. A. Parsegian. 1998. Lipid packing stress and polypeptide aggregation: alamethicin channel probed by proton titration of lipid charge. *Faraday Discuss.* 111: 173–183.

Borukhov, I., D. Andelman, and H. Orland. 1997. Steric effects in electrolytes: a modified Poisson–Boltzmann equation. *Phys. Rev. Lett.* 79:435–438.

Borukhov, I., D. Andelman, and H. Orland. 1998. Random polyelectrolytes and polyampholytes in solution. *Eur. Phys. J. B.* 5:869–880.

Cullis, P. R., M. J. Hope, B. de Kruijff, A. J. Verkleij, and C. P. S. Tilcock. 1985. Structural properties and functional roles of phospholipids in biological membranes. *In* Phospholipid and Cellular Regulation, vol. 1., J. F. Kuo (ed.). CRC Press, Boca Raton, FL. 1–59.

de Kruijff, B. 1997. Lipid polymorphism and biomembrane function. *Curr. Opin. Chem. Biol.* 1:564–569.

Epand, R. M. 1998. Lipid polymorphism and protein–lipid interactions. *Biochim. Biophys. Acta.* 1376:353–368.

Fattal, D. R., and A. Ben-Shaul. 1994. Mean-field calculations of chain packing and conformational statistics in lipid bilayers: comparison with experiments and molecular dynamics studies. *Biophys. J.* 67:983–995.

Flory, P. J. 1969. Statistical Mechanics of Chain Molecules. Wiley Interscience, New York.

Gawrisch, K., V. A. Parsegian, D. A. Hadjuk, M. W. Tate, S. M. Gruner, N. L. Fuller, and R. P. Rand. 1992. Energetics of a hexagonal-lamellar-hexagonal-phase transition sequence in dioleoylphosphatidylethanolamine membranes. *Biochemistry.* 31:2856–2864.

Gruen, D. W. R. 1981. A statistical mechanical model of the lipid bilayer above its phase transition. *Biochim. Biophys. Acta.* 595:161–183.

Gruen, D. W. R. 1985. A model for the chains in amphiphillic aggregates. 1. Comparison with a molecular dynamic simulation of a bilayer. *J. Phys. Chem.* 89:146–153.

Gruner, S. M. 1989. Stability of lyotropic phases with curved surfaces. *J. Phys. Chem.* 93:7562–7570.

Helfrich, W. 1973. Elastic properties of lipid bilayers: theory and possible experiments. *Z. Naturforsch.* 28C:693–703.

Henry, N. F. M., and K. Lonsdale. 1969. (eds.) International Tables for X-Ray Crystallography. Kynoch, Birmingham, U.K.

Hope, M. J., and P. R. Cullis. 1980. Effects of divalent cations and pH on phosphatidylserine model membranes: A ^{31}P NMR study. *Biochem. Biophys. Res. Comm. 92:846–852.*

Hui, S. K., 1997. Curvature stress and biomembrane function. *Curr. Topics Membranes.* 44:541–563.

Israelachvili, J. N. 1985. Intermolecular and Surface Forces. Academic Press, San Diego.

Jacobs, R. E., and S. H. White. 1989. The nature of the hydrophobic bonding of small peptides at the bilayer interface: implications for the insertion of transbilayer helices. *Biochemistry.* 28:3421–3437.

Kirk, G. L., S. M. Gruner, and D. L. Stein. 1984. A thermodynamic model of the lamellar to inverse hexagonal phase transition of lipid membrane-water system. *Biochemistry.* 23:1093–1102.

Kirk, G. L., and S. M. Gruner. 1985. Lyotropic effects of alkanes and headgroup composition on the $L_\alpha - H_{II}$ lipid liquid crystal phase transition: hydrocarbon packing versus intrinsic curvature. *J. Physique.* 46:761–769.

Kozlov, M. M., S. Leiken, and R. P. Rand. 1994. Bending, hydration and interstitial energies quantitatively account for the hexagonal-lamellar-hexagonal re-entrant phase transition in dioleoylphosphatidylethanolamine. *Biophys. J.* 67:1603–1611.

Landau, E. M., and J. P. Rosenbusch. 1996. Lipidic cubic phases: a novel concept for the crystallization of membrane proteins. *Proc. Natl. Acad. Sci. USA.* 93:14532–14535.

Leermakers, F. A. M., and J. M. H. M. Scheutjens. 1988. Statistical thermodynamics of association colloids. I. Lipid bilayer membranes. *J. Chem. Phys.* 89:3264–3274.

Leermakers, F. A. M., J. M. H. M. Scheutjens, and J. Lyklema. 1990. Statistical thermodynamics of association colloids. IV. Inhomogeneous membrane systems. *Biochim. Biophys. Acta.* 1024:139–151.

López Cascales, J. J., J. García de la Torre, S. J. Marrink, and H. J. C. Berendsen. 1996. Molecular dynamics simulation of a charged biological membrane. *J. Chem. Phys.* 104:2713–2720.

Marcelja, S. 1974. Chain ordering in liquid crystals. II. Structure of bilayer membranes. *Biochim. Biophys. Acta.* 367:165–176.

Markin, V. S., M. M. Kozlov, and V. L. Borovjagin. 1984. On the theory of membrane fusion. The stalk mechanism. *Gen. Physiol. Biophys.* 5:361–377.

Matsen, M. W., and M. Schick. 1994. Stable and unstable phases of a diblock copolymer melt. *Phys. Rev. Lett.* 72:2660–2663.

Matsen, M. W. 1995. Stabilizing new morphologies by blending homopolymer with block-copolymer. *Phys. Rev. Lett.* 74:4225–4228.

Mattice, W. L., and U. W. Suter. 1994. Conformational Theory of Large Molecules: The Rotational Isomeric State Model in Macromolecular Systems. Wiley-Interscience, New York.

Meijer, L. A., F. A. M. Leermakers, and A. Nelson. 1994. Modelling of electrolyte ions–phospholipid layers interaction. *Langmuir.* 10: 1199–1206.

Müller, M., and M. Schick, 1998. Calculation of the phase behavior of lipids. *Phys. Rev. E.* 57:6973–6978.

Rand, R. P., and N. L. Fuller. 1994. Structural dimensions and their changes in a reentrant hexagonal-lamellar transition of phospholipids. *Biophys. J.* 66:2127–2138.

Rand, R. P., and V. A. Parsegian. 1989. Hydration forces between phospholipid bilayers. *Biochim. Biophys. Acta.* 1031:1–69.

Seddon, J. M., G. Cevc, and D. Marsh. 1983. Calorimetric studies of the gel-fluid ($L_\alpha - L_\beta$) and lamellar-inverted hexagonal ($L_\alpha - H_{II}$) phase transitions in dialkyl- and diacylphosphatidylethanolamines. *Biochemistry.* 22:1280–1289.

Seddon, J. M., G. Cevc, R. D. Kaye, and D. Marsh. 1984. X-ray diffraction study of the polymorphism of hydrated diacyl- and dialkylphosphatidylethanolamines. *Biochemistry.* 23:2634–2644.

Seddon, J. M. 1990. Structure of the inverted hexagonal (H_{II}) phase, and non-lamellar phase transitions of lipids. *Biochim. Biophys.* 1031:1–69.

Shyamsunder, E., S. M. Gruner, M. W. Tate, D. C. Turner, P. T. C. So, and C. P. S. Tilcock. 1988. Observation of inverted cubic phase in hydrated dioleoylphosphatidylethanolamine membranes. *Biochemistry.* 27: 2332–2336.

Siegel, D. P. 1993. Energetics of intermediates in membrane fusion: comparison of stalk and inverted micellar intermediate mechanisms. *Biophys. J.* 65:2124–2140.

Steenhuizen, L., D. Kramer, and A. Ben-Shaul. 1991. Statistical thermodynamics of molecular organization in the inverse hexagonal phase. *J. Phys. Chem.* 95:7477–7483.

Tate, M. W. and S. M. Gruner. 1989. Temperature dependence of the structural dimensions of the inverted hexagonal (H_{II}) phase of phosphatidylethanolamine-containing membranes. *Biochemistry.* 28:4245–4253.

Tieleman, D. P., S. J. Marrink, and H. J. C. Berendsen. 1997. A computer perspective of membranes: molecular dynamic studies of lipid bilayer systems. *Biochim. Biophys. Acta.* 1331:235–270.